

PIB-PET SEGMENTATION FOR AUTOMATIC SUVR NORMALISATION WITHOUT MR INFORMATION

Parnesh Raniga^{1,2}, Pierrick Bourgeat¹,
Sébastien Ourselin¹

¹BioMedIA Lab, AS Laboratory,
CSIRO ICT Centre,
Brisbane, Australia

² Department of Electrical
and Information Engineering,
The University of Sydney,
Sydney, Australia

Victor Villemagne³, Graeme O'Keefe³,
Christopher Rowe³

³Department of Nuclear Medicine and
Centre for PET, Austin Hospital,
Melbourne, Australia

ABSTRACT

Pittsburg Compound B (PIB) is a Positron Emission Tomography (PET) radio tracer used to image *in-vivo*, beta amyloid plaques which are one of the major histopathological hallmarks of Alzheimer's disease (AD). Quantitative analysis of PIB retention requires normalisation of the PIB uptake values, to allow inter and intra subject comparisons. The standard uptake value ratio (SUVR) normalises the uptake values to the mean uptake value within a region containing non-specific binding, the cerebellar grey matter in the case of PIB. SUVR calculations are normally performed manually on the PET image by neurologist which is time consuming and non-reproducible. In this study, we present an automatic technique to extract the cerebellar grey matter on PET images, and validate its accuracy for SUVR normalisation on a database of 45 subjects.

Index Terms— SUVR, PIB PET, PET Segmentation

1. INTRODUCTION

With the advances in medicine and technology, the average lifespan of individuals is rapidly increasing. The prevalence of Alzheimer's disease (AD) in the population increases with age, doubling for every five years in age after the age of 65. Over the age of 80, the rate of AD is above 20% [1, 2]. This presents a substantial burden on the health system and deterioration in the quality of life of the subjects. To prevent, treat and better manage AD, its pathogenesis needs to be understood and measured both qualitatively and quantitatively.

Although the cause of AD is yet to be determined, currently its definitive diagnosis can only be obtained after post-mortem confirmation of pathologies such as high deposition of beta amyloid ($A\beta$) plaques and neuro fibrillary tangles in the cortical grey matter of the subjects. Histological studies

with analogous results have lead to the postulation of the amyloid cascade hypothesis (ACH) which states that the build up of $A\beta$ plaques in the cortical grey matter of subjects is a precursor to AD and leads to neuronal loss and cognitive decline [3]. Subsequently the development of *in-vivo* techniques for quantitative and qualitative evaluation of the $A\beta$ plaque burden and related pathologies would aid the diagnosis of and research into AD.

The advent of biomarkers such as Pittsburg Compound B (PIB) for PET gives the ability to image and evaluate, *in-vivo*, the $A\beta$ burden [4]. Qualitative monitoring of plaque build-up and quantitative analysis of PIB PET will provide significant indications as to the validity of the ACH and insight into the pathogenesis of AD, potentially leading to early diagnosis. However before quantitative analysis of PIB uptake can be performed, normalisation of the PIB uptake values to allow inter and intra subject comparisons has to be made. In clinical practice a normalization for the radioactive dose and the patients mass or volume, the standard uptake value (SUV), is performed. However for inter-subject comparison the SUV is not an accurate measure.

A more accurate normalisation technique is the distribution volume ratio (DVR) which is commonly used for normalising PET images of PIB and other radio ligands. DVR is the ratio of the distribution volume (DV) of a region to a reference region. The reference region is generally chosen to be one that does not contain receptors and therefore, has only non-specific binding. The DV, which is related to the number of binding sites can be calculated by applying a standard two or three compartment model which requires arterial sampling or dynamic acquisition.

Studies have shown that PIB does not specifically bind to the diffuse plaques in the cerebellar grey matter [5] hence SUVR, with the cerebellar grey matter as the reference re-

gion, can be used as a normalization technique. Lopresti *et al* [6] have shown that SUVR and DVR provide similar discrimination on a 20 minute acquisition, 40 minutes post injection, between AD and control cases. Since SUVR does not require arterial sampling and is easier to calculate, it has become the method of choice for normalising PIB PET images in clinical settings.

Brain tissue uptake values are normalised against the mean value obtained within the cerebellar grey matter region. Albeit faster and easier than DVR, SUVR normalisation is still performed manually and can be time consuming particularly when a large number of cases need to be processed. An automated SUVR calculation is desirable not only to accelerate the process but to reduce the variability inherent in manual techniques.

The first step in any automated technique would be the delineation of a suitable cerebellar grey matter region. Due to the low resolution and the lack of structural information in PET images, previous works on delineation of volumes of interest (VOI) on PET images have mainly focused on propagating a labeled atlas to the subjects MR first, using affine and non-rigid registrations, and then propagating it to the subjects PET image [7, 8]. Yasuno *et al* [9] enhanced this approach using segmented MR grey matter (GM) and white matter (WM) masks to restrict the VOIs. Svarer *et al* [10] proposed to warp multiple manually segmented MRs to the subjects MR to generate probability maps and produce individualised VOIs. However, these techniques rely on the availability of the MR scan, which are not always acquired in a clinical setting as it is time consuming and costly.

Without the availability of MR information, Yasuno's approach could be adapted to PET images through the segmentation of the PET image itself. For segmentation of PET images, most methods in literature are based on modelling the tracer uptake in dynamic fluorodeoxyglucose (FDG) PET images. Wong *et al* applied a k-means algorithm to dynamic PET images [11], while Kim *et al* [12] used a combination of region growing with cluster analysis to combine spatial and temporal information. However, such methods are not appropriate for PIB as high variability exists in tracer uptake between normal controls and AD subjects, and the introduction of a model without accurate diagnosis of the subject would bias results. A hybrid approach which enforces anatomical constraints while estimating the tissue classifications from the data is required therefore we applied the Expectation Maximisation (EM) approach of Van Leemput *et al* [13] to the segmentation of the PIB PET images into GM, WM and cerebrospinal fluid (CSF). The proposed approach uses the results of the PET segmentation to automatically extract the cortical GM of the cerebellum. The aim was to develop a fast and robust algorithm for SUVR calculation using only PET images. Results are compared against manual delineation and the straight propagation of the labelled atlas on the PET image using affine registration.

2. MATERIALS AND METHODS

2.1. Subjects and Data Acquisition

As a part of a study into AD and the use of PIB PET as an early indicator of AD, 45 subjects were scanned. Of the subjects, 13 were classified as AD (6 male and 7 female, mean age 73.85 ± 11.69), 6 as Mild Cognitive Impaired (MCI) (6 female, mean age 70.67 ± 12.13) and 26 were Normal Controls (NC) (13 male and 13 female, mean age 71.88 ± 6.69). Scans were conducted on Phillips Gemini and Phillips Allegro PET scanners. The subjects were scanned for 20 minutes, 40 minutes post injection. SPGR MR scans were also conducted on 35 subjects.

2.2. PET Segmentation

Segmentation of the PIB PET images were conducted using a C++ implementation of Van Leemput's EM tissue classification algorithm. Gaussian distribution of the voxel intensities in each class is assumed and parameter estimation and refinement performed at each iteration of the algorithm. To restrict the search space and prevent misclassification, *a priori* knowledge in the form of probability maps for each of the three different tissue classes is used. The probability maps also enforce spatial consistency in anatomical structure on the segmentation and reduce the effects of variability in uptake within the GM. Normal controls have a consistent uptake with the GM whereas AD subjects have a much higher uptake in the frontal lobe GM with a decrease across the temporal and parietal lobes which can cause clustering approaches to fail.

Amyloid build up is a continuous process and intra-subject tracer uptake within identical classifications can be substantially different. Anatomical constraints alone can not compensate for this variability which require an extra correction step. Van Leemput's algorithm was originally developed for MR segmentation and models the bias field present in MR images as a linear combination of smoothly varying polynomial basis functions estimating the bias at each iteration of the EM loop. Although no bias field exists in a PET image, the same scheme can be used to model the variability in tracer concentration as these variations are typically of low frequency with no abrupt changes. Estimation of the variability from the images allows for compensation on a per subject basis. To aid the segmentation a Markov random field (MRF) is used to provide consistency and noise reduction.

To enforce anatomical consistency, *a priori* probability maps and Montreal Neurological Institute (MNI) Single Subject (SS) template from the Statistical Parametrical Mapping (SPM) toolbox were used. An affine registration was performed between the template and PET or MR image using a robust block matching algorithm that has been previously validated on single and multi-modal registrations[14]. Subsequently, visual comparisons and Dice Similarity Coefficient (DSC) calculations were conducted for binary GM and WM segmenta-

tions of PET images with regard to resampled MR segmentations.

2.3. SUVR Calculation

For manual calculation, a cerebellar grey matter region was delineated by a neurologist on each PET scan. A cerebellar grey matter region was also delineated on the MNI SS template.

Mean calculations from the manual delineations were used as ground truth and compared against the following automated techniques.

- **Straight propagation of cerebellar mask onto PET image (SP)**

The MNI SS template was affinely registered to the PET image, and the cerebellar grey matter region was propagated to the PET image.

- **Propagation of cerebellar mask constrained using PET segmentation (CP)**

The GM mask from the PET segmentation was used to constrain the cerebellar mask by only considering voxels which were non-zero in both masks.

An error metric, defined as

$$\frac{ABS(Mean_a - Mean_m)}{Mean_m} \times 100 \quad (1)$$

where $Mean_a$ is the calculated mean from the automated method and $Mean_m$ is that of the manual delineation, was calculated for each of the automated methods. All calculations were performed using the Insight Registration and Segmentation Toolkit (ITK).

3. RESULTS AND DISCUSSION

3.1. PET Segmentation

Sagittal slices from PET and MR segmentations of NC and AD subjects are presented in Fig. 1. The PET and MR segmentations are similar despite the difference in resolution and tracer concentration variability in the PET images between the subjects.

Average DSC of the PET GM and WM segmentation with regards to MR segmentations are shown in Table. 1. Due to the low resolution of PET resulting in Partial Volume Effects (PVEs), the DSCs are low. Partial Volume Effects are caused due to an imaged structure being smaller than twice the resolution of the scanner resulting in blurring of signal from the structure. Low resolution and PVEs cause contours to be blurred and details lost culminating in differences between MR and PET segmentation. However the scores compare favourably against those presented in [12] who performed a similar comparison for their segmentation algorithm.

Improvements in segmentation results could be achieved by restricting the bias field estimation to GM regions as they contain the most variability, and tailoring the *a priori* probability maps for atrophy present in AD subjects.

Classification	GM	WM
	M-DSC \pm STD	M-DSC \pm STD
AD	0.56 \pm 0.07	0.65 \pm 0.09
MCI	0.59 \pm 0.04	0.69 \pm 0.04
NC	0.52 \pm 0.05	0.63 \pm 0.07

Table 1. Mean DSC (M-DSC) and standard deviation (STD) of the PET GM and WM segmentation with regards to the MR segmentation

3.2. SUVR Calculation

Mean error for both the SP and CP techniques are presented in Table. 2. Errors in CP technique were between 4.5 and 8.6 percent. Errors for the AD class of subjects were higher than those of the other classes due to strong atrophy and variation in tracer concentration. Since comparisons were made against manual delineations, any inherent error and variability in them would adversely affect the results. Errors were also introduced during the registration steps both when the PET image is being segmented and when the reference mask is being propagated. Although the segmentation algorithm compensates for minor misregistrations, any registration errors during reference mask propagation will adversely affect the results.

Improvements to the variance and error can be made by adapting the bias field, *a priori* maps and templates for cerebellum only segmentation since SUVR calculations require only cerebellar grey matter. Ideally the cerebellum would be parcellised and segmented separately to prevent bias introduced in the bias field estimation as a result of variations in other regions. Robustness of the current technique can be improved by parcellising the cerebellum and restricting calculations to be within the parcellisation thus negating registration errors and differences in anatomy. The algorithms have a running time of less than 3 and 6 minutes respectively for the SP and CP techniques.

Classification	ME \pm STD	ME \pm STD
	(SP)	(CP)
AD	15.39% \pm 8.62%	8.63% \pm 6.68%
MCI	16.91% \pm 5.74%	4.53% \pm 2.70%
NC	15.48% \pm 8.75%	5.73% \pm 4.73%

Table 2. Mean error (ME) and standard deviation (STD) for the SP and CP techniques.

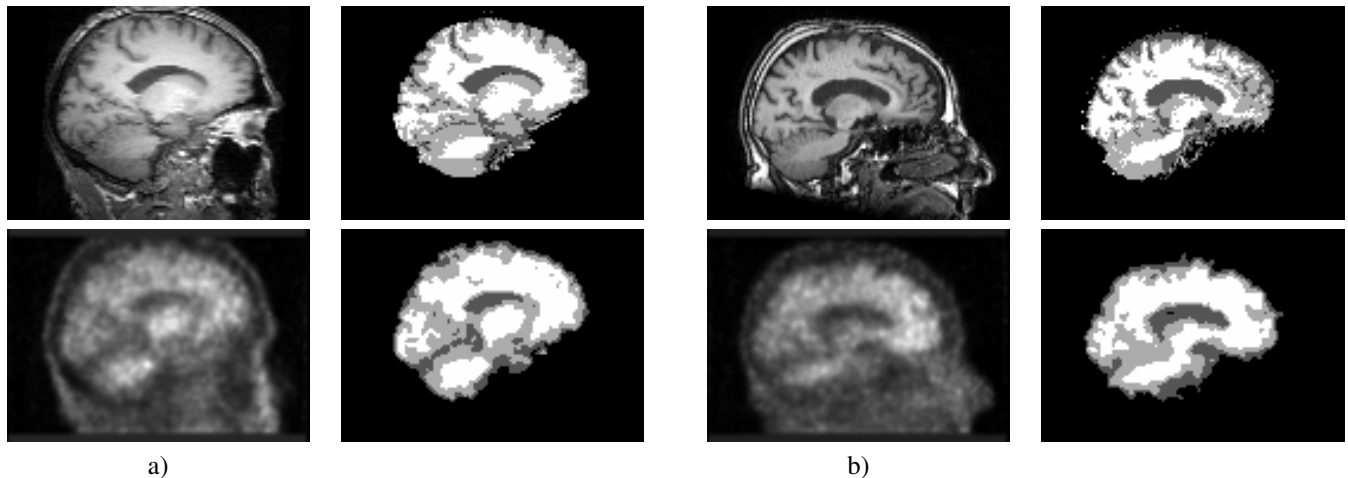


Fig. 1. Sagittal slices of MR (top row) and PIB PET (bottom row) of a NC subject (a) and an AD subject (b). Combined GM, WM and CSF segmentation results are presented right of the original scans.

4. CONCLUSION

We have presented an automatic, fast (less than 6 minutes), PET based SUVR calculation technique. We have compared results of the algorithm with results from manual delineations and straight propagation using affine registration.

Further improvements in SUVR calculation by adapting the bias field for better estimation of tracer variability are being investigated. Specific *a priori* data for the different classes of subjects are also being investigated along with restriction of the segmentation within the cerebellum. Another avenue for future work is a PET based cerebellar parcellisation technique. Such a technique would prevent the need for the propagation of masks thus avoiding registration errors and would improve the robustness of the current technique. Both these techniques would reduce variance in SUVR values due to variances in subject scans as they are tailored for individual subjects.

5. REFERENCES

- [1] A. Wimo and B. Winblad *et al*, "The magnitude of dementia occurrence in the world," *Alzheimer Dis Assoc Disord*, vol. 17, no. 2, pp. 63–67, Apr-Jun 2003.
- [2] L. Fratiglioni and L.J. Launer *et al*, "Incidence of dementia and major subtypes in Europe: A collaborative study of population-based cohorts. neurologic diseases in the elderly research group," *Neurology*, vol. 54, no. 11 Suppl 5, pp. 10–15, 2000.
- [3] J. Hardy and D.J. Selkoe, "The amyloid hypothesis of Alzheimer's disease: progress and problems on the road to therapeutics," *Science*, vol. 297, no. 5580, pp. 353–356, Jul 2002.
- [4] W.E. Klunk and H. Engler *et al*, "Imaging brain amyloid in Alzheimer's disease with Pittsburgh Compound-B," *Ann Neurol*, vol. 55, no. 3, pp. 306–319, Mar 2004.
- [5] W.E. Klunk and Y. Wang *et al*, "The binding of 2-(4'-methylaminophenyl)benzothiazole to postmortem brain homogenates is dominated by the amyloid component," *J Neurosci*, vol. 23, no. 6, pp. 2086–2092, Mar 2003.
- [6] B.J. Lopresti and W.E. Klunk *et al*, "Simplified quantification of Pittsburgh Compound B amyloid imaging PET studies: a comparative analysis," *J Nucl Med*, vol. 46, no. 12, pp. 1959–1972, Dec 2005.
- [7] A. Hammers and M.J. Koepp *et al*, "Implementation and application of a brain template for multiple volumes of interest," *Hum Brain Mapp*, vol. 15, no. 3, pp. 165–174, Mar 2002.
- [8] A. Hammers and R. Allom *et al*, "Three-dimensional maximum probability atlas of the human brain, with particular reference to the temporal lobe," *Hum Brain Mapp*, vol. 19, no. 4, pp. 224–247, Aug 2003.
- [9] F. Yasuno and A.H. Hasnine *et al*, "Template-based method for multiple volumes of interest of human brain PET images," *Neuroimage*, vol. 16, no. 3 Pt 1, pp. 577–586, Jul 2002.
- [10] C. Svarer and K. Madsen *et al*, "MR-based automatic delineation of volumes of interest in human brain PET images using probability maps," *Neuroimage*, vol. 24, no. 4, pp. 969–979, Feb 2005.
- [11] K-P Wong and D. Feng *et al*, "Segmentation of dynamic PET images using cluster analysis," *IEEE Trans Nucl Sci*, vol. 49, no. 1, pp. 200–207, Feb. 2002.
- [12] J Kim and W. Cai *et al*, "Segmentation of VOI from multi-dimensional dynamic PET images by integrating spatial and temporal features," *IEEE Trans Inf Technol Biomed*, vol. 10, no. 4, pp. 637–646, Oct 2006.
- [13] K. Van Leemput and F. Maes *et al*, "Automated model-based tissue classification of MR images of the brain," *IEEE TMI*, vol. 18, pp. 897–908, 1999.
- [14] S. Ourselin and A. Roche *et al*, "Reconstructing a 3D structure from serial histological sections," *IVC*, vol. 19, pp. 25–31, 2001.